Medical Image Analysis 20 (2015) 224–236

Contents lists available at ScienceDirect

Medical Image Analysis

journal homepage: www.elsevier.com/locate/media

Non-invasive evaluation of breast cancer response to chemotherapy using quantitative ultrasonic backscatter parameters

Lakshmanan Sannachi [a,b], Hadi Tadayyon [a,b], Ali Sadeghi-Naini [a,b], William Tran [a], Sonal Gandhi [c], Frances Wright [d], Michael Oelze [e], Gregory Czarnota [a,b,*]

[a] Department of Radiation Oncology, and Physical Sciences, Sunnybrook Health Sciences Centre, Toronto, ON, Canada
[b] Department of Radiation Oncology and Medical Biophysics, University of Toronto, Toronto, ON, Canada
[c] Division of Medical Oncology, Sunnybrook Health Sciences Centre, Toronto, ON, Canada
[d] Division of General Surgery, Sunnybrook Health Sciences Centre, Toronto, ON, Canada
[e] Bioacoustics Research Laboratory, Department of Electrical and Computer Engineering, University of Illinois, Urbana-Champaign, USA

ARTICLE INFO

Article history:
Received 3 February 2014
Received in revised form 14 November 2014
Accepted 17 November 2014
Available online 25 November 2014

Keywords:
Breast cancer
Chemotherapy
Quantitative ultrasound
Scattering property
Clinical response

ABSTRACT

Tumor response to neoadjuvant chemotherapy in patients ($n = 30$) with locally advanced breast cancer (LABC) was examined using quantitative ultrasound. Three ultrasound backscatter parameters, the integrated backscatter coefficient (IBC), average scatterer diameter (ASD), and average acoustic concentration (AAC), were estimated from tumors prior to treatment and at four times during neoadjuvant chemotherapy treatment (weeks 0, 1, 4, 8, and prior to surgery) and compared to ultimate clinical and pathological tumor responses. Results demonstrated that among all parameters, AAC was the best indicator of tumor response early after starting treatment. The AAC parameter increased substantially in treatment-responding patients as early as one week after treatment initiation, further increased at week 4, and attained a maximum at week 8. In contrast, the backscatter parameters from non-responders did not show any changes after treatment initiation. The two patient populations exhibited a statistically significant difference in changes of AAC ($p < 0.001$) and ASD ($p = 0.023$) over all treatment times examined. The best prediction of treatment response was achieved with the combination of AAC and ASD at week 4 (82% sensitivity, 100% specificity, and 86% accuracy) of 12–18 weeks of treatment. The survival of patients with responsive ultrasound parameters was higher than patients with non-responsive ultrasound parameters (35 ± 11 versus 27 ± 11 months, respectively, $p = 0.043$). This study demonstrates that ultrasound parameters derived from the ultrasound backscattered power spectrum can potentially serve as non-invasive early measures of clinical tumor response to chemotherapy treatments.

1. Introduction

1.1. Locally-advanced breast cancer

One of the most common types of cancer diagnosed in women is breast cancer (American Cancer Society, 2013). Women with locally-advanced breast cancer (LABC) have poor long-term survival rates compared to early stage patients (5 year survival rate of ~55%) (Giordano, 2003). LABC comprises a wide range of clinical scenarios including T3/T4 disease tumor, includes tumor sized greater than 5 cm, and disease often involving the skin and chest wall with extensive axillary lymph node involvement. Standard therapy for LABC is multimodality treatment. This often starts with neoadjuvant chemotherapy to permit tumor shrinkage and metastatic control (typically mastectomy, sometime lumpectomy), and followed by surgery and then radiation therapy. However, LABC treatment remains controversial due to uncertainties in the optimization of treatment methodology (Esteva and Hortobagyi, 2008). Complete pathological response to chemotherapy treatment predicts good patient survival. Several studies demonstrated the importance of clinical and pathologic complete response to neoadjuvant chemotherapy as an indicator of a better outcome (Chollet et al., 1997; Smith et al., 2002). The early detection of treatment response of breast tumors is very important in order to be able to guide cancer therapy decisions based on individual patient responses (Esteva and Hortobagyi, 2008).

Clinical imaging techniques including mammography, CT, and magnetic resonance imaging (MRI) have been typically used for

* Corresponding author at: Department of Radiation Oncology, and Imaging Research – Physical Science, Sunnybrook Health Sciences Centre, 2075 Bayview Avenue, Suite T2-185, Toronto, ON M4N 3M5, Canada. Tel.: +1 416 480 6100x7073; fax: +1 416 480 6002.
E-mail address: Gregory.Czarnota@sunnybrook.ca (G. Czarnota).

http://dx.doi.org/10.1016/j.media.2014.11.009
1361-8415/

assessments of patient responses to cancer therapy based on anatomical tumor size measurements, typically months after treatment. However, changes in tumor size with cancer treatment are often the late cumulative result of early micro-structural changes in tumor cell morphology due to cell death, which start to take place within hours to days after treatment initiation. An imaging modality which can assess significant changes in cell-death related tumor micro-structure would be advantageous for the early assessment of treatment response and could facilitate the change of ineffective treatments early (within days), rather than having a patient subjected to months of an ineffective treatment.

1.2. Ultrasound imaging of biological tissues

Ultrasonic imaging has seen an increase in its utilization for diagnostic and therapeutic purposes over the last 50 years. It is highly sensitive to variations in micro-structural properties of tissues at many size scales. Ultrasound scattering is caused by differences in density and/or compressibility relative to the surrounding tissue across the ultrasound wave's propagation region. Backscattered acoustic signals from biological tissues contain information about the size, shape, number, and relative acoustic impedance of scattering regions within the tissues (Feleppa et al., 1997). The most popular way of displaying backscatter information is B-mode imaging. This technique uses the envelope of detected ultrasound echoes from a region of interest to typically create gray-scale images which display a cross-sectional map of the echo intensity. However, these images only use a fraction of the information contained in the signal. Several investigators have suggested that the frequency dependent information in ultrasonic echo signals can be related to acoustical and structural properties of tissue microstructure (Feleppa et al., 1986; Lizzi et al., 1988; Lizzi et al., 1997a, 1997b). The radio frequency (RF) spectrum of ultrasound backscatter signals has since been used in various tissue characterization applications such as the diagnosis of ocular tumors, examinations of liver and renal tissues, prostate cancer, and studies of cardiac and vascular abnormalities (Feleppa et al., 1997; Guimond et al., 2007; Lizzi et al., 1997a, 1997b; Yang et al., 2007). In most of these studies, spectral parameters were extracted from ultrasonic backscatter signals and related to specific pathological alternations of the investigated specimens. Those spectral parameters are mid-band fit, spectral slope, and 0-MHz intercept which are related to scatterer shape, size and acoustic concentration (product of number concentration of scatterer and the relative impedance difference between the scatterer and surrounding tissues) (Lizzi et al., 1988, 1997a, 1997b). These parameters are calculated from the linear regression analysis of backscatter power spectrum. More complex parameters are described below.

1.3. Cancer response monitoring using ultrasound

Treatments such as neoadjuvant chemotherapy for LABC patients can alter the structural and mechanical properties of tumor tissues. Tumor cell death is characterized often by nuclear condensation and fragmentation, and also features significant changes in cell structure and cellular organization. Tumor degeneration in response to treatment also exhibits considerable interactions with stromal cells (Schedin et al., 2007). All of these are expected to alter ultrasonic backscatter. In an *in vitro* ultrasound based non-invasive monitoring of epithelial cell death study, results demonstrated a reasonable correlation of spectral slope and integrated backscatter coefficient, which were extracted from ultrasound power spectra, to apoptotic cell death (Brand et al., 2009). In different cancer therapy response monitoring studies, high frequency quantitative ultrasound (20–50 MHz) was initially used to detect changes in tissue microstructure due to a variety of cancer therapies *in vitro*, in situ and *in vivo* (Banihashemi et al., 2008; Czarnota et al., 1999, 2012; Lee et al., 2012; Vlad et al., 2009, 2008). Other studies used high frequency quantitative ultrasound to detect apoptotic cell death in tumors treated with photodynamic therapy, X-ray radiation, and ultrasonically activated anti-vascular microbubble treatments in a variety of *in vivo* mouse models. Those studies demonstrated up to 16-fold maximal increases in observed backscatter signal intensity accompanied by changes in spectral parameters. Recently, in studies of treatment response monitoring in breast cancer xenograft tumors (Sadeghi-Naini et al., 2013a) and clinical breast tumors treated with chemotherapy (Sadeghi-Naini et al., 2013b) using low-frequency clinical range (7 MHz) quantitative ultrasound spectral parameters, responding tumors demonstrated approximately up to a 7 to 12 – fold maximal increase in mid-band fit and 0-MHz intercept and 8 to 9 – fold maximal increases in mid-band fit and 0-MHz intercept after cancer therapy initiation.

1.4. Backscatter parameter estimation for tissue characterization

Acoustic scattering theories for biological tissues assume that tissues can be modeled as low density of random scatterers (Oelze and Zachary, 2006; Oelze et al., 2004, 2002). Since there are a large number of interdependent properties embedded in backscatter signals, it is difficult to extract estimates of individual properties accurately without simplifying assumptions. The average scatterer size and average acoustic concentration which reflect tissue microstructure observed from microscopic optical histological evaluation can be estimated from backscatter signals by assuming their shape, organization and elastic properties of scatterers in the medium (Oelze et al., 2002, 2004). This ultrasonic backscatter parameter estimation technique has been used to classify tissue abnormalities compared to normal tissues and to differentiate one tumor type from another. In those studies, several types of nonlinear frequency-dependent scattering models have been utilized to describe tissue micro-structure including the Gaussian, fluid-filled sphere, and spherical-shell models (Feleppa et al., 1997; Insana and Hall, 1990; Oelze and O'Brien, 2006). Among them, backscatter parameters estimated using the fluid-filled sphere model (FFSM) have demonstrated reasonable correlations with tissue micro-structure (Oelze and O'Brien, 2006). The quantitative ultrasound parameters used in the previous studies for tissue characterization are listed below in Table 1 with their proper definition and tissue features which determine the value of each parameter.

Previously, observational tumor response monitoring studies have been conducted with retrospective analyses of patient outcomes in breast cancer patients receiving chemotherapy treatment, using elastography and quantitative ultrasound imaging techniques (Falou et al., 2013; Sadeghi-Naini et al., 2013b). Specifically, strain ratios and strain differences in elastography, and spectral parameters in quantitative ultrasound have been correlated to treatment response. In the study here, the integrated backscatter coefficient and two individual structural properties such as average scatterer size and average acoustic concentration were determined from ultrasonic backscatter signals. These are used here for the first time to monitor micro-structural alternations within tumors in 30 LABC patients after chemotherapy treatment and to evaluate whether the patients have been responsive or not to their treatments. The FFSM was used to extract backscatter properties from breast tumors over a frequency bandwidth of 4.5–9 MHz. The clinical-response –based survival curve, which is determined months later at the time of surgery has been presented in this study in order to highlight the importance of treatment with tumor response in comparison therapy without response, since the lack of such response can significantly impact patient survival.

Table 1
Quantitative ultrasound parameters with their definition and corresponding tissue features which determine the value of each parameter.

Parameters and definition	Corresponding tissue features
Spectral parameters: Derived from the backscatter power spectrum by linear regression analysis over the frequency bandwidth (Lizzi et al., 1988, 1997a, 1997b)	
Mid-band fit (MBF) [dB]: Value of the linear fit at the center frequency	Scatterer size, shape, number, organization and their elastic properties
0-MHz intercept (SI) [dB]: Extrapolation of linear regression of spectrum at 0 MHz	Scatterer size, shape, number, organization and their elastic properties
Spectral slope (SS) [dB/MHz]: Slope of the linear regression of spectrum over the bandwidth	Scatterer size and shape
Backscatter Parameters: Derived from backscatter coefficients by fitting with theoretically derived backscatter coefficient using a scatterer model over frequency bandwidth (Insana and Hall, 1990)	
Integrated backscatter coefficient (IBC) [dB]: Integration of the backscatter coefficient within the bandwidth of the transducer	Scatterer size (ASD), shape, number, organization and their elastic properties
Average Scatterer Diameter (ASD) [μm]: Estimated by comparing scatterer model function to that measured for the sample using a least-squares method	Scatter size may be cell size or cellular ensembles dependent on the ultrasound wavelength
Average Acoustic concentration (AAC) [dB/cm^3]: It is the coefficient of the fitted backscatter coefficient. It is defined as the product of number concentration of scatterers times the relative impedance difference between the scatterers and surrounding tissues	Scatterer number density, organization and their elastic properties

Associated ultrasonic-backscatter-parameter-based survival curves have been presented to show the potential of early quantitative ultrasound in assessing of breast tumor response as linked to patient survival. The results demonstrate that backscatter parameters extracted from ultrasound data are predictive of ultimate clinical chemotherapy response, as early as 1 week after treatment initiation. Based on such observation clinicians can potentially customize cancer therapies, and thereby change ineffective treatment within days to weeks of starting therapy, instead of continuing for several months only to find no patient benefit and be faced with little or no options for recourse.

2. Materials and methods

2.1. Study protocol and patient characteristics

Thirty LABC patients were examined in this study in accordance with institutional research ethics guidelines. Before treatment all patients underwent a core needle biopsy to confirm a cancer diagnosis, where the tumor grade and histological subtype were recorded. In addition MRI scanning of the breast was performed clinically to determine initial tumor size and disease extent. The breast tumor was examined by clinicians at each time after treatment and post-treatment MRI scans of the breast were also acquired immediately before patient surgery to measure any residual tumor size. Following patients' operations mastectomy specimens were examined by a board-certified pathologist using whole-mount $5'' \times 7''$ pathology slides digitized using a confocal scanner (TISSUEscope™, Huron Technologies, Waterloo, ON) (Clarke et al., 2007). Patient characteristics, tumor properties, as well as treatments administered are summarized in Table 2. The patients had an average age of 47 ± 8 years (range: 33–62 years). The average tumor size was 7.3 ± 3.3 cm (range: 1.9–14 cm). Among thirty patients, 29 patients had invasive ductal carcinoma and one had metaplastic carcinoma. Patients were followed clinically after their treatment with a mean follow-up period of 35 ± 10 months (range: 15–50 months) for recurrence-free survival. Clinical pathological responses of the patients are given in Table 3. Patients were classified as responders or non-responders based on their ultimate clinical and pathological response. A "good" response was defined by an over 50% diminishment in tumor size (compared to pretreatment size) along with reasonable decreases in tumor cellularity, and a "poor" response was defined as less than 50% diminishment in tumor size accompanied by no significant changes in tumor cellularity. Patients ($n = 23$) were classified as good responders due to the absence of tumor or presence of only minimal invasive disease, after neo-adjuvant chemotherapy. Patients 3, 8, 12, 13, 24, 27 and 28 had a poor pathological response. Their tumor sizes were minimally changed compared to their pretreatment size. Patients 2 and 18 were exceptional cases in that the reduction in tumor size was less than 50%, however, since the residual tumor cellularity was very low, these patients were clinically/pathologically classified as responders.

2.2. Ultrasound data acquisition

Breast tumor ultrasound scanning was directed by an oncologist. Ultrasonic data were acquired from breast tumor volumes before treatment, at week 1, 4 and 8 after start of treatment, in addition to prior to surgery, which typically occurred 12–18 weeks after last cycle of the treatment. But, same number of patient could not be maintained over all time points due to the absence of the patient (compliance with scans and physician appointments). Specifically, the number of patients examined before treatment, at weeks 1, 4, 8 after treatment and, prior to surgery were 30 (23 responders and 7 non-responders), 29 (22 responders and 7 non-responders), 29 (22 responders and 7 non-responders), 26 (20 responders and 6 non-responders), and 20 (15 responders and 5 non-responders), respectively. All ultrasonic breast imaging and RF data acquisition were performed with a Sonix RP clinical system operating with L14-5/60 Transducer of center frequency 7 MHz (Ultrasonix, Vancouver, Canada) and −6 dB bandwidth range from 4.5 to 9 MHz. RF data were sampled at 40 MHz. Each image frame was stored with 512 RF lines over a 6 cm width and 4–6 cm depth. Four to seven images planes were acquired at 1 cm intervals across breast tumors, with the transducer focus set at the midline of the tumor. Scan focal depths remained consistent for individual patients throughout the study.

2.3. Backscatter parameter estimations

Backscatter parameters were derived from estimates of the backscatter coefficient $\sigma_m(f)$, which is defined as the differential scattering cross section per unit solid angle at 180°, per unit volume. Backscatter coefficients are estimated from a normalized power spectral density of the ultrasound echo signal using the equation

$$\sigma_m(f) = \frac{1.45R_1^2}{A_0\Delta z}\left(\frac{\gamma'}{2}\right)^2 \frac{|S_m(f,Z_l)|^2}{|S_0(f,Z_l)|^2} e^{-4(\alpha_m(f)-\alpha_0(f)(R_1+\frac{\Delta z}{2}))} \quad (1)$$

where f is frequency in MHz, A_0 is the area of the transducer aperture. $S_m(f)$ and $S_0(f)$ are the Fourier transform of the sample and reference echo signals respectively. α_m and α_0 are the sample

Table 2
Patient characteristics.

Patient No.	Age	Menopausal Status	Pretreatment Tumor Dimension (APxMLxSI) in cm	Histology	Grade	ER/PR	Her-2-neu	Neoadjuvant treatment
1	55	Postmenopausal	5.4 × 5 × 2.3	ductal	I	–	+	FEC + paclitaxel, trastuzumab
2	53	Postmenopausal	7.4 × 7	ductal	II	+	–	Epirubicin, docetaxel
3	41	Premenopausal	4	ductal	III	+	+	Docetaxel, carboplatin, trastuzumab
4	50	Premenopausal	4 × 5	ductal	III	–	+	AC + docetaxel, trastuzumab
5	33	Premenopausal	3 × 3	ductal	I	+	–	AC + paclitaxel
6	33	Premenopausal	5.4 × 5 × 8	ductal	N/A	+	+	AC + docetaxel, paclitaxel, trastuzumab
7	48	Postmenopausal	4.9 × 4.9 × 4.1 and 3.2 × 1.3 × 2.9	ductal	II	+	–	AC + docetaxel
8	36	Premenopausal	4.4 × 3.9 × 5.8	ductal	II	+	–	AC + paclitaxel
9	40	Premenopausal	4.4 × 3.4	ductal	III	–	–	AC + paclitaxel
10	62	Postmenopausal	12 × 14	ductal	III	–	–	FEC + docetaxel
11	59	Postmenopausal	6 × 2.3 × 4.3	ductal	II	–	–	AC + paclitaxel
12	38	Premenopausal	7.5 × 4.9 × 9.2	ductal	II	+	–	AC + paclitaxel
13	53	Postmenopausal	8.4 × 9.4 × 12.7	metaplastic	III	–	–	AC + cisplatinum, gemcitabine platinum
14	50	Premenopausal	13 × 11	ductal	III	–	–	AC + paclitaxel
15	49	Premenopausal	7.1 × 5.5 × 8.9	ductal	III	–	+	Docetaxel, trastuzumab
16	40	Premenopausal	3 × 2.4 × 3	ductal	III	+	+	AC + paclitaxel, trastuzumab
17	56	Postmenopausal	2.4 × 2.7 × 3.2	ductal	II	–	+	AC + paclitaxel, trastuzumab
18	47	Premenopausal	5.2 × 4 × 4	ductal	II	+	–	FEC + docetaxel
19	52	Postmenopausal	4.1 × 3 × 2.5	ductal	II	+	–	AC + docetaxel, paclitaxel
20	44	Premenopausal	9.9 × 4.5 × 9.7	ductal	II	+	+	AC + paclitaxel, trastuzumab
21	38	Premenopausal	9 × 6.6 × 6	ductal	II	+	–	AC + paclitaxel
22	58	Postmenopausal	1.9 × 1.4 × 1.6	ductal	III	–	–	AC + paclitaxel
23	38	Premenopausal	8 × 8	ductal	III	–	+	Dose-dense AC + paclitaxel, trastuzumab
24	47	Premenopausal	8 × 10	ductal	II	+	–	Dose-dense AC + paclitaxel
25	57	Postmenopausal	7.9 × 4.1 × 5.5	ductal	III	–	–	Dose-dense AC + paclitaxel
26	47	Premenopausal	6.3 × 4.1 × 7.4	ductal	N/A	–	+	Dose-dense AC + paclitaxel, trastuzumab
27	55	Premenopausal	6.6 × 12.8 × 6.8	ductal	II	+	–	AC + paclitaxel
28	38	Premenopausal	2.3 × 2.5 × 2.5 and 1.0 × 1.0 × 0.7	ductal	III	–	–	AC + paclitaxel
29	59	Postmenopausal	8 × 5.7 × 3	ductal	II	+	+	FEC + docetaxel, trastuzumab
30	50	Premenopausal	9 × 7 × 3	ductal	II	+	–	AC + paclitaxel

AC, adriamycin and cytoxan; FEC, 5-fluorouracil, epirubicin and cyclophosphamide.

Table 3
Patient pathological response results.

Patient No.	Post treatment Tumor Dimension (APxMLxSI) in cm	Notes	Pathological Response
1	N/A	Complete pathological response	Good
2	7 × 5 × 3	Carcinoma with mucinous features; Very low cellularity	Good
3	2.7 × 2.5 × 2.4	Tumor cellularity remains very high	Poor
4	N/A	Complete pathological response	Good
5	1.4	Good response	Good
6	N/A	Complete pathological response	Good
7	1.4 × 1 × 1	Small volume of invasive tumor remaining	Good
8	11.4	Extensive residual disease	Poor
9	N/A	Complete pathological response, with only fibrous tumor bed remaining	Good
10	N/A	Complete pathological response	Good
11	2.6 × 2.5 × 2.5	Good response	Good
12	6.5 × 3 × 7.3	Invasive ductal carcinoma remaining	Poor
13	All the breast	Residual tumor took up all the breast; no response	Poor
14	4	Good response	Good
15	2 × 1.5 × 1	Complete pathological response, with only in situ disease remaining	Good
16	0.2 × 0.2	Complete pathological response, with only in situ disease remaining	Good
17	0.2 × 0.2	Very good response	Good
18	6.5	Exceedingly low cellularity, thus overall tumor volume is also very low	Good
19	1 × 0.7 × 0.6	Complete pathological response, with only in situ disease remaining	Good
20	2 × 1 × 1 and 1.6 × 1 × 0.5	Good response, tumor cellularity is low	Good
21	2.9 × 2 × 1.5 and 2 × 1.5 × 1	Tumor cellularity is low	Good
22	N/A	Complete pathological response, with only fibrous tumor bed remaining	Good
23	N/A	Complete pathological response	Good
24	12.5 × 4.5 × 3.5	No definite response	Poor
25	N/A	No residual invasive carcinoma in the breast, only lymphovascular invasion remaining	Good
26	N/A	Complete pathological response, only scattered in-situ component remaining	Good
27	17	No definite response	Poor
28	2.8 × 3.0 × 2.3 and 1.5 × 1.6 × 1.1	No definite response	Poor
29	N/A	Complete pathological response	Good
30	1.2	Small volume of invasive tumor remaining	Good

and reference medium attenuation values, respectively. Δz is the axial length of the range gated volume, and R_1 is the on-axis distance between the transducer and proximal surface of the gated volume. γ' is the amplitude reflection coefficient of reference plane reflector.

However, this equation can only be used to estimate BSC from power spectrum obtained from single-element transducers. For clinical ultrasound applications, where linear array transducer are used, a reference phantom technique was used to account for clinical system dependencies in backscatter coefficient estimation (Yao et al., 1990) as shown in Eq. (2). In that technique, the system dependent effects such as system transfer function, transducer beam forming, and diffraction artifacts were removed by normalizing the backscatter power spectra calculated from the tumor region to the corresponding reference spectra calculated from reference phantom whose backscatter coefficient (σ_r) and attenuation coefficient (α_r) were determined using absolute measurement methods (Madsen et al., 1999). The attenuation of the entire breast for all patients was estimated to be 1 dB/MHz/cm based on data reported in literature (Berger et al., 1990; Duric et al., 2005).

$$\frac{\sigma_m(f)}{\sigma_r(f)} = \frac{|S_m(f)|^2}{|S_r(f)|^2} e^{4(\alpha_m(f)-\alpha_r(f)(R_1 L+\frac{\Delta z}{2}))} \tag{2}$$

where $S_r(f)$ and $\sigma_r(f)$ are the Fourier transform of the reference phantom echo signals and corresponding backscatter coefficient respectively. RF Signal analysis and backscatter coefficient estimation was performed off-line using a custom-made MATLAB (Mathworks, Natick, MA, USA) program. This program enabled the visualization of the RF data similar to a B-mode image and was used to select a region-of-interest. For the estimation of ultrasound backscatter parameters, the ROIs were selected from each image plane for each tumor sample and averaged for the final analysis. The RF lines were analyzed using a sliding window algorithm. A Hanning window function of length 10 times the wavelength of the center frequency with an 80% overlap between adjacent windows in axial direction and 60 scan lines laterally was used. The breast tumor BSC, $\sigma_m(f)$ was calculated from their corresponding power spectrum of the gated RF signal from each ROI as shown in Eq. (2).

First, the integrated backscatter coefficient (IBC) was calculated by integrating the backscatter coefficient within the bandwidth of the transducer (Machado and Foster, 2001). It is related to the micro-structural properties of tumor such as scatterer size, shape, number and scatterer randomization. Estimates of the average scatterer properties such as average scatterer diameter (ASD) and average acoustic concentration (AAC) were calculated by comparing the calculated BSC, $\sigma_m(f)$ of the gated RF signal from each ROI over frequency bandwidth to a theoretically derived backscattered coefficient, $\sigma_{theor}(f)$ using a least squares method (Insana and Hall, 1990)

$$\sigma_{theor}(f) = Cf^4 a_{eff}^6 n_z F(f, a_{eff}) \tag{3}$$

where constant $C = \pi^2/36c^4$ and c is the speed of sound in the medium, n_z is scatterer acoustic concentration and F is the form factor which describes the backscatter coefficient as a function of frequency. In this study, the FFSM was used with the assumption of invasive duct carcinoma cells as scatterers and connective tissues as a surrounding medium to extract backscatter parameters from breast tumors. The mean square error (MSE) value which indicates the goodness of fit between measured and a theoretically derived backscatter coefficient was also calculated. Finally, QUS parametric images were constructed by superimposing colored pixels, whose colors were associated with QUS parameter estimate values and locations associated with the sliding window locations, on the original grey scale B-mode image of the tumor (Insana and Hall, 1990).

2.4. Statistical analysis

Changes in the backscatter parameters values between responders and non-responders and also within the treatment time points were compared using analyses of variance (ANOVA) followed by Bonferroni multicomparison test. Changes in the backscatter parameter values from baseline between responders and non-responders at each time point for backscatter parameters were also compared independently. Discriminant analysis was used to determine which backscatter parameter discriminated between responders and non-responders at weeks 1, 4, and 8, and 1 week prior to surgery. The changes in the values of backscatter parameters were used as predictors in the analysis, which examined the best separation between the two groups. Sensitivity and specificity were calculated to quantify the performance of the classification method in terms of discriminating responders from non-responders. Survival rate for two treatment response populations were created by the Kaplan–Meier method to clarify the time dependent cumulative survival rate, and the curves were compared using the log-rank test. $P < 0.05$ was considered to determine a statistically significant difference.

3. Results

3.1. Backscatter property evaluation of treatment response

Ultrasound B-mode images and backscattered RF data were collected for each patient before and at specified times during treatment. Chemotherapy treatment produced consistent and reproducible changes in ultrasound images and backscatter parameters as a function of time after treatment. Backscatter coefficient (BSC) changes over the −6 dB bandwidth of the transducer for both the responder and non-responder cases are shown in Fig. 1a and b and the IBC parameter was calculated within this bandwidth. The FFSM was used to extract AAC and ASD parameters from the measured BSC for each region-of-interest (ROI), which was selected in the tumor region.

Representative ultrasound B-mode images and the QUS backscatter parametric images acquired from a responding and non-responding patient with LABC tumor prior to chemotherapy onset and four weeks after start of treatment are presented in Fig. 1c and d. An overall increase in the ultrasound backscatter power was detected within the tumor region and also in the AAC parametric images in responders. No such changes were observed in the non-responding patients. Parametric images of the ASD did not present any changes over the course of treatment in any of the patient populations. Representative light microscopy images of whole-mount histopathology samples obtained following mastectomy are presented in Fig. 2. In the non-responding patient, glandular tumor cell structure was relatively uniform in size and shape and distributed as solid sheets of cells throughout the tumor and large amounts of residual carcinoma were present. In the responding patient shown, scant cells appeared randomly distributed in the extracellular matrix throughout the tumor with minimal residual disease present.

Representative backscatter parametric images for a clinically responding and a non-responding patient acquired before treatment, at weeks 1, 4, and 8, and preoperatively are presented in Fig. 3a–c, respectively. Responders and non-responders demonstrated similar backscatter parameter values before treatment with a mean IBC of $0.13 \pm 0.18 \times 10^{-4}$, and $0.11 \pm 0.11 \times 10^{-4}$ Sr^{-1} cm^{-1}, respectively, a mean AAC of 67 ± 5, and 68 ± 5 dB/cm^3, respectively, and a mean ASD of 109 ± 6, and 113 ± 3 μm, respectively. The range of ASD estimates using the FFSM agreed generally well with the

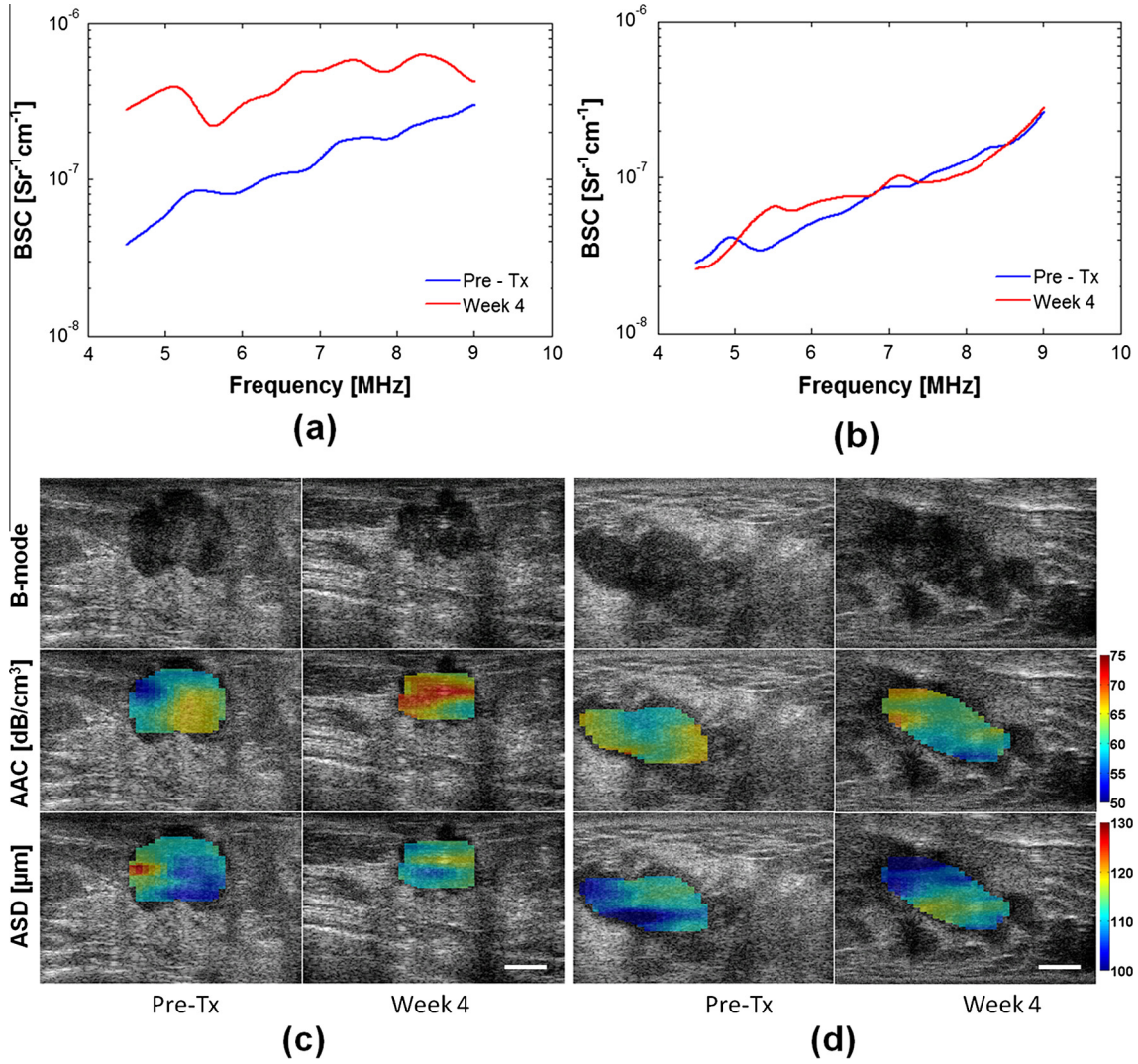

Fig. 1. Backscatter coefficient plots from responder (a) and non-responder (b). B-mode and parametric images of AAC and ASD images from a responding (c) and a non-responding breast tumor (d) before starting neo-adjuvant chemotherapy (Pre-Tx) and after 4 weeks of treatment (Week 4). Color bars for AAC and AAC correspond to values given beside them. The white scale bar represents 10 mm.

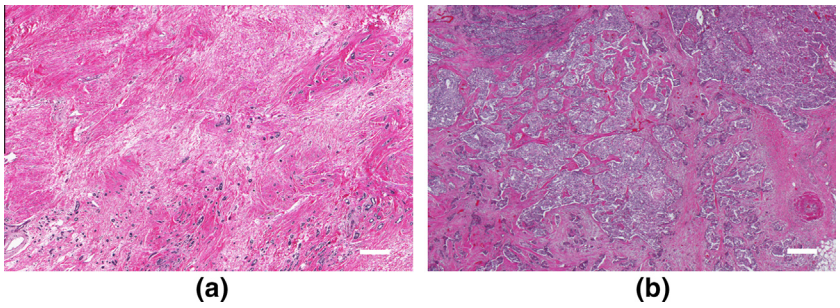

Fig. 2. Light microscope images of whole mount histopathology from responder (a) and non-responder (b) with high magnifications. In the responding tumor, carcinoma is completely destroyed by the chemotherapy treatment. In the non-responding tumor, a large residual carcinoma deposit remaining is shown.

gland diameters (range: 52–118 µm) observed from histopathology images of the breast tumors.

Average changes in IBC, AAC and ASD parameters estimated for the responders and non-responders over the treatment period are presented in Fig. 4. The IBC parameters increased during treatment to a maximum of $1.71 \times 10^{-4}\,\mathrm{Sr}^{-1}\,\mathrm{cm}^{-1}$ in responders at week 8. Analysis using ANOVA with a Bonferroni correction demonstrated significant differences in changes of IBC between those values acquired at weeks 1 and 8 in responders. In contrast, the IBC parameter from non-responders did not show any changes after treatment initiation. The two patient populations exhibited a statistically significant difference in changes of IBC only at week 1

of treatment ($p = 0.032$). Like IBC, the AAC parameters increased after treatment in responding patients and obtained a maximum of 6.9 dB/cm^3 at week 8. In addition, analysis with ANOVA demonstrated significant differences in changes of AAC between those values acquired at week 1 and 8 in responder population. This parameter from non-responders was relatively static at all times after treatment. The two patient populations exhibited a statistically significant difference in changes of AAC at week 4 ($p < 0.001$), week 8 ($p = 0.008$), and at week 1 ($p = 0.007$) of chemotherapy. The ASD parameter in responders or non-responders did not appear to be affected by clinical tumor response. Analysis with ANOVA showed significant differences in changes of the backscatter parameters, AAC, and ASD between the two response populations over all treatment groups. Pre-operative scans were acquired 12–18 weeks after the last cycle of the chemotherapy (typically 5–6 months after the start of treatment). At that time since the chemotherapy has been stopped for several weeks at this stage, it is expected that there is minimal active chemotherapy induced cell death. Also the complete pathological responders (with no tumor discernible on ultrasound), and hence who have no residual tumor left clinically for imaging or for analysis, are excluded from the averaged data at this time. All of these factors contribute to a different parameter value at the pre-op stage as compared to week 8. Therefore, backscatter parameters estimated from pre-operative scans were not included for statistical analysis (Table 4).

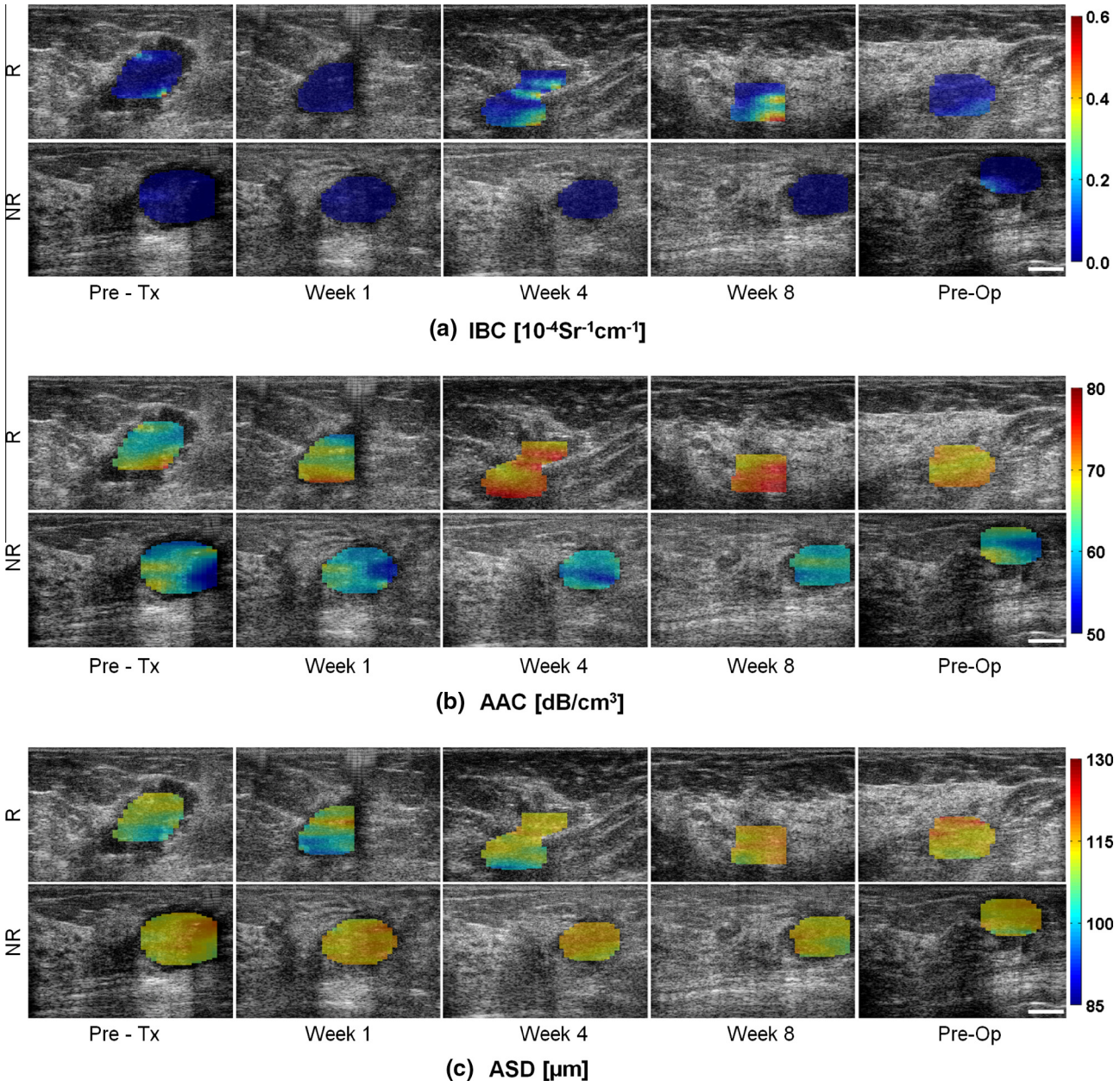

Fig. 3. Representative parametric images of IBC (a), AAC (b), and ASD (c) from a responding (N) and non-responding (NR) patient. The data for each patient was acquired from the same nominal region, prior to treatment (Pre-Tx), as well as at weeks 1, 4 and 8 during treatment times, and pre-operatively (Pre-Op, 12–18 weeks after treatment initiation), from left to right, respectively. But, same number of patient could not be maintained over all time points due to the absence of the patient (compliance with scans and physician appointments). Specifically, the number of patients examined before treatment, at weeks 1, 4, 8 after treatment and, prior to surgery were 30 (23 responders and 7 non-responders), 29 (22 responders and 7 non-responders), 29 (22 responders and 7 non-responders), 26 (20 responders and 6 non-responders), and 20 (15 responders and 5 non-responders), respectively. The white scale bar represents ~10 mm.

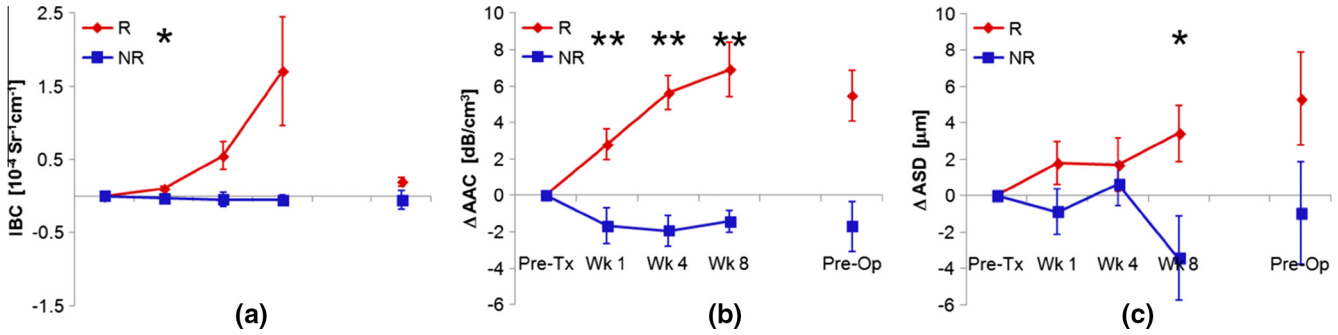

Fig. 4. Average change in IBC (a), AAC (b) and ASD (c) parameters measured in clinically treatment responders and non-responders over treatment time. Error bars represent the mean ± one standard error. ** ($p < 0.005$) and * ($p < 0.05$) represents the significant different based on ANOVA test. R: Responder; NR: Non-Responder; Pre-Tx: Pretreatment; Pre-Op: Preoperation.

Table 4
Summary of p values obtained from statistical tests of significance carried out for changes in backscatter parameters using ANOVA test over treatment times for both responder and non-responder and also over treatment responses.

Parameters	Over treatment time		Over responses			
	R	NR	Week 1	Week 4	Week 8	Overall
IBC	0.028*	0.822	0.032*	0.096	0. 221	0.069
AAC	0.031*	0.739	0.007*	0.000†	0.008*	0.000†
ASD	0.636	0.166	0.269	0.694	0.029*	0.023*

* Statistically significant ($p < 0.05$).
† Statistically highly significant ($p < 0.0001$).

3.2. Classification of survival analysis

In order to classify the two patient populations based on their ultimate clinical/pathological response to the treatment, linear discriminant analysis was performed on the changes in the backscatter parameters estimated at weeks 1, 4, and 8, and the week prior to surgery. Among all three estimated backscatter parameters, the AAC was the dominant parameter in terms of achieving the best classification results for the two patient populations at all times (Table 5). The best linear discriminant analysis based predictor of treatment response was obtained with the linear combination of AAC and ASD parameters at 4 weeks (81.8% sensitivity, 100% specificity and 86.2% accuracy) followed by the one obtained using a combination of AAC and ASD at week 8 (80% sensitivity, 100% specificity and 84.6% accuracy) and with less sensitivity using the combination of all backscatter parameters at week 1 (77.3% sensitivity, 85.7% specificity and 79.3% accuracy). The linear discriminant models for a two patient population classification at weeks 1, 4, and 8 are shown in Eq. (4). All the responders and non-responders are predicted with a classifier score of positive and negative values, respectively. Overall, the combination of AAC and ASD was found to be the best predictor of treatment response at all times after starting treatment. A reasonable linear discriminant analysis-based predictor of treatment response was obtained for the combined data (including weeks 1, 4, and 8) with linear combination of AAC and ASD (77% sensitivity, 95% specificity and 81% accuracy) and the corresponding model is shown in Eq. (5). Fig. 5 presents a feature plot of the change in ASD versus the change in AAC parameters where the threshold to discriminate ultrasound-responsive and non-responsive patients in this study is determined by discriminant analysis and has been indicated by a dashed line.

Kaplan–Meier curves for chemotherapy treatment response based on clinical-pathological response and linear discriminant models derived using ultrasonic backscatter parameters acquired at week 1, 4, and 8 after treatment are presented in Fig. 6. The survival rate of the pathological responders was significantly higher than that of the non-responders ($p = 0.001$). Whereas the estimated backscatter parameters could classify responders and non-responder population with an accuracy of 79% at week 1, the survival rate of those two populations did not show a significant difference ($p = 0.318$). Results of the survival study demonstrated a higher survival rate for the ultrasound responding patients compared to the non-responding patients, identified based on ultrasonic backscatter parameters at week 4 ($p = 0.043$) and week 8 ($p = 0.037$) after treatment initiation.

$$\begin{aligned} ClassifierScore_{Wk1} &= -0.28 + 0.06ASD_{Wk1}\ \mu m + 0.24AAC_{Wk1}\ dB\ cm^{-3} \\ &\quad + 3.64IBC_{Wk1}10^{-4}\ Sr^{-1}\ cm^{-1} \\ ClassifierScore_{Wk4} &= -1.14 + 0.13ASD_{Wk4}\ \mu m + 0.53AAC_{Wk4}\ dB\ cm^{-3} \\ ClassifierScore_{Wk8} &= -0.76 + 0.21ASD_{Wk8}\ \mu m + 0.28AAC_{Wk8}\ dB\ cm^{-3} \end{aligned} \quad (4)$$

$$\begin{aligned} ClassifierScore_{Combined} &= -0.6 + 0.12ASD_{Combined}\ \mu m \\ &\quad + 0.31AAC_{Combined}\ dB\ cm^{-3} \end{aligned} \quad (5)$$

4. Discussion

Clinical imaging techniques such as MRI, CT and mammography have been typically used for assessment of patient responses to

Table 5
Discrimant analysis at week 1, 4 and 8.

Parameters	Week 1			Week 4			Week 8		
	Sens.	Spec.	Accu.	Sens.	Spec.	Accu.	Sens.	Spec.	Accu.
IBC	56	100	66	32	100	48	25	100	42
AAC	68	86	72	82	100	86	75	100	82
ASD	50	71	55	50	57	51	70	83	73
IBC, AAC	73	100	79	82	100	86	75	100	82
IBC, ASD	73	86	76	59	100	69	80	83	82
AAC, ASD	73	86	76	82	100	86	80	100	85
IBC, AAC, ASD	77	86	79	82	100	86	80	100	85

cancer therapy based on anatomical tumor size measurements, usually after treatment. Nevertheless, it can take up to several weeks to a few months to assess treatment response based on physical size measurements since size changes are often late indicators of response. Several studies have demonstrated the potential of early assessments of tumor response at days to weeks for adaptive treatment modification, since changes in tissue at a microscopic level start to occur early after cancer therapy (Esteva and Hortobagyi, 2008; Huang et al., 2002). The ultrasonic backscatter parameter characterization technique used in this study is sensitive to such changes in tissue structure and tissue mechanical properties at a microscopic level.

4.1. Breast cancer response monitoring using ultrasonic backscatter parameters

In this study, we report for the first time the results of a clinical investigation on 30 patients with LABC receiving neoadjuvant chemotherapy, whose tumor responses were monitored using QUS backscatter parameters with a 7 MHz clinical ultrasound device. The FFSM was applied here for the first time to extract individual tissue scatterer properties like scatterer size and acoustic concentration from clinical *in vivo* breast tumor data in order to determine if estimates of scatterer properties could be related to tissue microstructure changes and to distinguish clinically responding and non-responding patients. Use of the FFSM permitted fairly good differentiation of responders and non-responders. Compared to macroscopic stiffness estimation using elastography techniques (Falou et al., 2013) or general ultrasonic spectral parameter investigation as in our previous studies (Sadeghi-Naini et al., 2013b), backscatter parameter estimation techniques provide more specific information about the tumor microstructure like scatter size and acoustic concentration at a microscopic level. Whereas the elastographic and ultrasound parameters investigated previously exhibited statistically significant differences between responder and non-responder populations after only 4 weeks of treatment, the backscatter parameters presented in this study showed promise in differentiating the treatment responding and non-responding patients as soon as 1 week after treatment, with statistical significance. In particular, statistically significant difference in the AAC parameter were observed at week 1 between two populations ($p = 0.027$). The AAC parameter is related to scatterer number density and scatterer mechanical properties (Feleppa et al., 1986). This finding suggests that changes in tissue microstructure in the breast tumor start to occur within 1 week from the initiation of treatment. Examining histopathology images of responding tumors suggest that as the tumor begins to respond to the treatment it undergoes various pathological changes including early cellular changes such as nuclear aggregation, condensation, and fragmentation (karyorrhexis and karyolysis) in tumor cells and fibrosis, collagenization, and microcalcification in the stroma (Sethi et al., 2012). Invasive ductal carcinoma cells in patients with complete response begin to die likely within 1–4 weeks after the start of chemotherapy, and are replaced with collagen and fibrotic deposition over the long term (months). The early cell-death related alterations in tissue microstructure are linked to significant changes in ultrasound parameters shortly after the start of treatment. The changes in structural and mechanical properties of the cancerous tissue can also lead to increases in acoustic scatterer concentration consistent with more nuclear fragmentation with cell death. The IBC ultrasound parameter is more dependent on scatterer size than acoustic scatterer concentration (Taggart et al., 2007). The ASD did not undergo any statistically significant changes at any time points after treatment. This would potentially explain why the IBC parameter did not result in statistically significant differences at treatment time points except at week 4 (discussed further below). In non-responder cases, tumors do not undergo significant cellular changes due to treatment. Therefore, the backscatter parameters

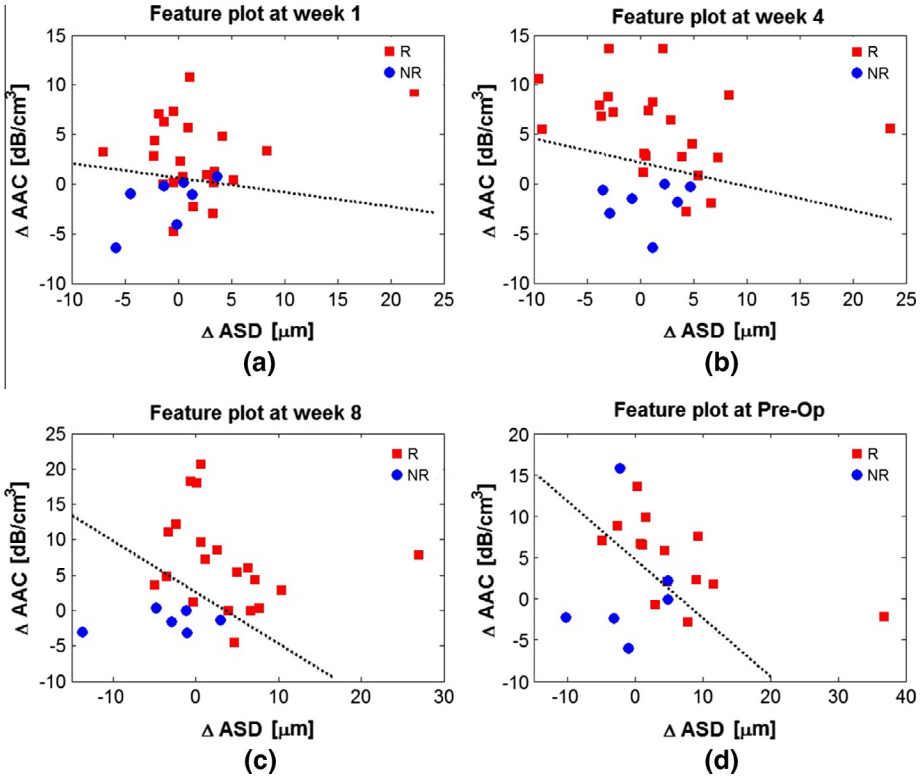

Fig. 5. Feature plots of the change in ASD versus the change in AAC data acquired at week 1 (a), week 4 (b) and week 8 (c) and the week prior to operation (d). Responders and non-responders have been classified via a linear discriminant analysis, where the determined threshold of classes has been demonstrated by dashed lines.

did not show any significant changes for these patient populations over treatment time. The reason for having a negative change in the IBC and AAC parameters in that group may be due to progressive disease identified in some of the non-responding patients, where the tumors tend to develop large necrotic cores after several cycles of therapy (necrotic cores were histologically identified post-mastectomy). The presence or development of necrotic cores may play a role in the decrease in IBC and AAC parameters for non-responders.

Linear discriminant analysis results here suggested a favorable classification and a promising separability of two patient populations using backscatter parameters acquired at weeks 1, 4, and 8 after chemotherapy initiation. In elastography studies, the sensitivity and specificity in discriminating responder and non-responder populations at best was 44% and 60%, respectively, at week 1, but increased to 100% and 100%, respectively, at week 4. In addition, tumor response can often be associated with inflammation which may confound elastography measurements (Falou et al., 2013). In the QUS spectral parameter estimation method, where the spectral parameters like mid-band fit, slope and intercept were calculated from ultrasound backscatter from tumor, the sensitivity and specificity at best was 83% and 100%, respectively, at week 4. However, it is noteworthy that the number of patients included in the previous studies of elastography and QUS spectroscopy was 15 and 24, respectively. On the other hand, the study here investigated the efficacy of the model-based backscatter parameters on 30 patients, thus potentially obtaining greater statistical power and better accounting for the heterogeneity of responses in breast tumors, compared to the previous studies. Here, a sensitivity and specificity of up to 82% and 100%, respectively, were obtained at week 4, and lesser values of 77% and 86% at week 1. Due to the small sample size, those specificity, sensitivity and accuracy values presented here are obtained by using the same training and test sets. The absence of independent test set results in optimistic estimations of the performance.

These promising results imply that QUS backscatter parameters can be potentially used for the early prediction of ultimate treatment response in patients undergoing cancer targeting therapies. Such an early prediction could be used to facilitate the critical decision of switching to a more effective therapy or salvage management for treatment of refractory patients early during a course of treatment instead of continuing an ineffective treatment for months.

Previous studies in cell and xenograft models have demonstrated that mid-to high-frequency ultrasound is sensitive in detecting cell death. The cellular nuclei are hypothesized to be the dominating source of scattering for this frequency range (Oelze and O'Brien, 2006). The interaction of ultrasound with biological tissue is determined by the mechanical properties of the underlying structure. In soft tissues, this structure is composed primarily of cellular matrix containing single cells in an aggregate. Ultrasonic scattering is caused by structures below and up to the order of the ultrasound wavelength. Thus, for the frequency range used in this study here, scatters are arranged as aggregates in the form of glands and lobules. Aggregates of cells arranged in the gland and lobules may undergo nuclear condensation and aggregation in response to chemotherapy (Fig. 7) as shown in (Banihashemi et al., 2008; Czarnota et al., 1999). These changes in cellular level predominantly affect only the ductal glands and lobules' mechanical properties, not their sizes. This would potentially explain why the ASD parameter is relatively invariant. Here, we have used a fluid filled sphere model for breast tumor

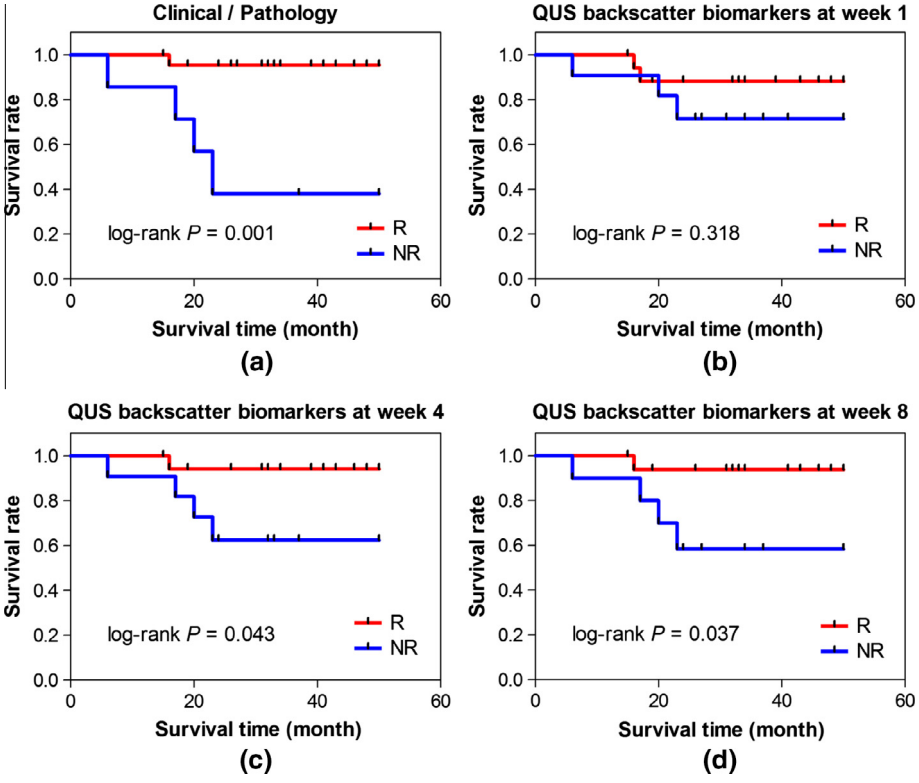

Fig. 6. Kaplan–Meier survival curves for chemotherapy treatment response based on clinical-pathological assessment (mean disease free survival responders 35 ± 11 months, mean survival non-responders 26 ± 11 months) (a) and ultrasonic backscatter parameters acquired at week 1 (b), week 4 (c), and week 8 (d) after treatment (mean disease free survival ultrasound-responsive patients 33 ± 11 months, mean survival ultrasound non-responsive patients 28 ± 12 months; mean disease free survival ultrasound-responsive patients 35 ± 11 months, mean survival ultrasound non-responsive patients 27 ± 11 months, mean disease free survival ultrasound-responsive patients 33 ± 10 months, mean survival ultrasound non-responsive patients 25 ± 12 months at weeks 1, 4, and 8, respectively.).

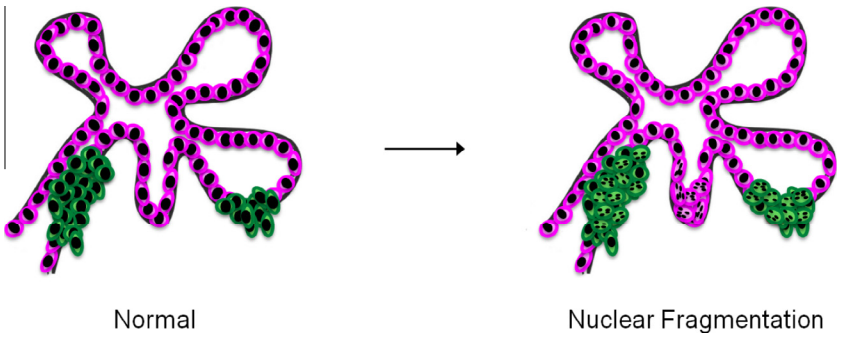

Fig. 7. Illustration of nuclear fragmentation within the tumor, induced by chemotherapy treatment.

ultrasound parameter determination. However, a model able to take into account more complex aggregates of fluid filled spheres or other structures may be beneficial in modeling the tumor response and improving the accuracy of response detection.

4.2. Further imaging modalities for monitoring tumor response to treatment

Currently, mammography is considered the primary imaging modality for breast screening. B-mode ultrasound imaging may also be used, depending on the mammogram findings. Breast tumor extent is better seen on mammograms and with more complex Dynamic Contrast Enhanced-MR images compared to B-mode ultrasound. Thus B-mode ultrasound is less often used for measuring tumor dimensions due to poor visibility of tumor margins. Anatomical imaging methods such as mammography, DCE-MRI, and ultrasound are typically used in the clinic for screening, pre-treatment assessment, and post-treatment assessment, and are rarely used to monitor the patient during the treatment (Giordano, 2003). There remains no clinically accepted functional imaging modality for early therapy response monitoring and other methods have exhibited variability. A previous study, which used DCE-MRI to measure early changes in breast tumor volume in response to chemotherapy treatment showed no significant changes after one cycle (3 weeks) despite positive clinical pathological response (Partridge et al., 2005). The modality used in that study was relatively insensitive in tissue imaging to cell function changes and requires the injection of exogenous contrast agent as a marker (Brindle, 2008). Typically, blood tests are only conducted prior to treatment in order to determine the suitability of patients for chemotherapy, and are not be used to predict treatment response. Diffuse optical imaging (DOI) is a relatively low resolution imaging technique which may cause uncertainties for identifying tumor region, especially in the case of small tumors (Falou et al., 2012; Soliman et al., 2010).

Several ultrasound methods have been explored in therapy response monitoring. Ultrasound Doppler imaging methods have been used to monitor tumor vascular disruption in real time following anti-vascular therapy by measuring blood flow velocity (Gee et al., 2001). Molecular imaging with ultrasound has recently involved the use of targeted intravascular microbubble contrast agents. Such large microbubbles however cannot leave the intravascular space and molecular imaging is limited in this compartment (Kaufmann and Lindner, 2007). Unlike these ultrasonic methods, the QUS backscatter based biomarkers investigated in this study depend on intrinsic contrast alternations arising from changes in the microstructure and elastic properties of cancer cells when they response to treatment, and hence the methods does not need contrast agent. Elastography, which measures tissue stiffness by detecting the effects of local tissue deformations, has been demonstrated recently in the classification of treatment responder and non-responder at week 4 after treatment initiation (Falou et al., 2013). Compared to the macroscopic stiffness estimation using this elastography method, this backscatter parameter estimation technique provides those tissue structural and mechanical properties at microscopic level. It may be confounded however by factors such as inflammation and DCIS which may also alter tissue stiffness. A genetic approach has been investigated recently for breast cancer therapy response monitoring by analyzing circulating tumor DNA (Dawson et al., 2013) specific to each tumor. Compared to this approach, QUS backscatter analysis as used in this study is rapid, inexpensive and a non-destructive method for cancer therapy response monitoring with signal changes universal for tumor response independent largely of tumor type. In our study, outcomes of patient treatment response classification based on the week 4 QUS backscatter parameter biomarkers matched with ultimate clinical and pathological response. Moreover, there were links based on ultrasound responsiveness to patient disease-free survival pointing to the utility of these ultrasound biomarkers to ultimate patient response to treatment and consequent survival.

5. Conclusions

In conclusion, specific information about tissue microstructure of breast tumors could be extracted from ultrasonic measurements using backscatter parameter estimation technique shown in this study compared to conventional B-mode ultrasound. We demonstrated that backscatter parameter estimates such as scatterer size and acoustic concentration may be used to monitor chemotherapy treatment response in breast tumors to discriminate between clinically responding and non-responding patients earlier during a course of treatment (weeks during treatment instead of months after treatment). This study was a "retrospective" observational study which did not affect patient treatment decisions. The aim of this study was to show the potential of early QUS-assessment of breast tumor response as an imaging therapy-response assessment tool. In keeping with this, the survival curves that are been presented in this study are done so in order to highlight the importance of an early prediction of ultimate treatment response, and show a linkage between ultrasound parameters ("biomarkers") of response and outcome. In the future, this may permit an objective rational change of an ineffective treatment to a more effective one, since lack of such response can significantly impact the ultimate survival of the cancer patients. Whereas the current number of participating patients seems reasonable for the proof of principle work carried out here, large cohort of patients in future, should improve the statistical power of this type of study. Invasive ductal carcinoma which is examined in this is highly pleomorphic in nature, which contains a broad variability in size and shape of the tissue microstructure. With the frequency range used in this study,

scattering structures include arterioles, mammary ducts and glands-any connective tissue structure rich in collagen, and elastin fibers (Cooper's ligaments). Thus, for a more accurate backscatter parameter estimation from treatment responding and non-responding breast tumors, more detailed scattering models with knowledge of acoustic impedance of subcellular, cellular, and glandular tissue in order to understand the contribution of each structural component of the tumor to the ultrasound signal at each frequency of analysis bandwidth would potentially improve results. Nevertheless, the findings here suggests that it may be possible to use this method to facilitate clinicians in making decisions to modify cancer therapies early on to better personalize cancer therapy.

Acknowledgements

This work was supported by the Natural Sciences and Engineering Council of Canada, Terry Fox New Frontiers Program Projects in Ultrasound for Cancer Therapy, Canadian Breast Cancer Foundation – Ontario Region, the Canadian Institutes of Health Research, the Canadian Foundation for Innovation, Ontario Ministry of Research and Innovation and Ryerson University. G.J.C. is an author on two issued patents 'Use of high frequency ultrasound imaging to detect and monitor the process of apoptosis in living tissues, ex vivo tissues and cell-culture' US patent #6511430 and a 'Method of monitoring cellular death using low frequency ultrasound' US patent #8192362 held by the Sunnybrook Health Sciences Centre (Toronto, ON, Canada). G.J.C. holds a Jim and Mry Davie Research Chair in Breast Cancer Imaging. A.S.N. holds a Banting Postdoctoral Fellowship, and held a Canadian Breast Cancer Foundation Postdoctoral Fellowship partly during the conduct of this research.

Appendix A. Supplementary material

Supplementary data associated with this article can be found, in the online version, at http://dx.doi.org/10.1016/j.media.2014.11.009.

References

American Cancer Society, 2013. Cancer Facts & Figures.

Banihashemi, B., Vlad, R., Debeljevic, B., Giles, A., Kolios, Michael, C., Czarnota, Gregory, J., 2008. Ultrasound imaging of apoptosis in tumor response: novel preclinical monitoring of photodynamic therapy effects. Cancer Res. 68, 8590–8596.

Berger, G., Laugier, P., Thalabard, J.C., Perrin, J., 1990. Global breast attenuation: control group and benign breast diseases. Ultrason. Imaging 12, 47–57.

Brand, S., Solanki, B., Foster, D.B., Czarnota, Gregory, J., Kolios, Michael, C., 2009. Monitoring of cell death in epithelial cells using high frequency ultrasound spectroscopy. Ultrasound Med. Biol. 35, 482–493.

Brindle, K., 2008. New approaches for imaging tumour responses to treatment. Nat. Rev. Cancer 8, 94–107.

Chollet, P., Charrier, S., Brain, E., Curé, H., Van Praagh, I., Feillel, V., De Latour, M., Dauplat, J., Misset, J.L., Ferrière, J.P., 1997. Clinical and pathological response to primary chemotherapy in operable breast cancer. Eur. J. Cancer 33, 862–866.

Clarke, G.M., Eidt, S., Sun, L., Mawdsley, G., Zubovits, J.T., Yaffe, M.J., 2007. Whole-specimen histopathology: a method to produce whole-mount breast serial sections for 3-D digital histopathology imaging. Histopathology 50, 232–242.

Czarnota, G.J., Kolios, M.C., Abraham, J., Portnoy, M., Ottensmeyer, F.P., Hunt, J.W., Sherar, M.D., 1999. Ultrasound imaging of apoptosis: high-resolution non-invasive monitoring of programmed cell death in vitro, in situ and in vivo. Br. J. Cancer 81, 520–527.

Czarnota, Gregory, J., Karshafian, R., Burns, P.N., Wong, S., Al Mahrouki, A., Lee, J.W., Caissie, A., Tran, W., Kim, C., Furukawa, M., Wong, E., Giles, A., 2012. Tumor radiation response enhancement by acoustical stimulation of the vasculature. Proc. Natl. Acad. Sci. USA 109, E2033–E2041.

Dawson, S.J., Tsui, D.W.Y., Murtaza, M., Biggs, H., 2013. Analysis of circulating tumor DNA to monitor metastatic breast cancer. N. Engl. J. Med. 368, 1199–1209.

Duric, N., Littrup, P., Babkin, A., Chambers, D., Azevedo, S., Kalinin, A., Pevzner, R., Tokarev, M., Holsapple, E., Rama, O., Duncan, R., 2005. Development of ultrasound tomography for breast imaging: technical assessment. Med. Phys. 32, 1375.

Esteva, F.J., Hortobagyi, G.N., 2008. Can early response assessment guide neoadjuvant chemotherapy in early-stage breast cancer? J. Natl Cancer Inst. 100, 521–523.

Falou, O., Sadeghi-Naini, A., Prematilake, S., Sofroni, E., Papanicolau, N., Iradji, S., Jahedmotlagh, Z., Lemon-Wong, S., Pignol, J.-P., Rakovitch, E., Zubovits, J., Spayne, J., Dent, R., Trudeau, M., Boileau, J.F., Wright, F.C., Yaffe, Martin, J., Czarnota, , Gregory, J., 2013. Evaluation of neoadjuvant chemotherapy response in women with locally advanced breast cancer using ultrasound elastography. Translational Oncol. 6, 17–24.

Falou, O., Soliman, H., Sadeghi-Naini, A., Iradji, S., Lemon-Wong, S., Zubovits, J., Spayne, J., Dent, R., Trudeau, M., Boileau, J.F., Wright, F.C., Yaffe, Martin, J., Czarnota, , Gregory, J., 2012. Diffuse optical spectroscopy evaluation of treatment response in women with locally advanced breast cancer receiving neoadjuvant chemotherapy. Translational Oncol. 5, 238–246.

Feleppa, E.J., Lizzi, F.L., Coleman, D.J., Yaremko, M.M., 1986. Diagnostic spectrum analysis in ophthalmology: a physical perspective. Ultrasound Med. Biol. 12, 623–631.

Feleppa, Ernest, J., Liu, Tian, Kalisz, A., Shao, M.C., Fleshner, N., Reuter, V., Fair, W.R., 1997. Ultrasonic spectral-parameter imaging of the prostate. Int. J. Imaging Syst. Technol. 8, 11–25.

Gee, M.S., Saunders, H.M., Lee, J.C., Sanzo, J.F., Jenkins, W.T., Evans, S.M., Trinchieri, G., Sehgal, C.M., Feldman, M.D., Lee, W.M., 2001. Doppler ultrasound imaging detects changes in tumor perfusion during antivascular therapy associated with vascular anatomic alterations. Cancer Res. 61, 2974–2982.

Giordano, S.H., 2003. Update on locally advanced breast cancer. Oncologist, 521–530.

Guimond, A., Teletin, M., Garo, E., D'Sa, A., Selloum, M., Champy, M.-F., Vonesch, J.-L., Monassier, L., 2007. Quantitative ultrasonic tissue characterization as a new tool for continuous monitoring of chronic liver remodelling in mice. Liver Int. 27, 854–864.

Huang, E., McNeese, M.D., Strom, E.A., Perkins, G.H., Katz, A., Hortobagyi, G.N., Valero, V., Kuerer, H.M., Singletary, S.E., Hunt, K.K., Buzdar, A.U., Buchholz, T.A., 2002. Locoregional treatment outcomes for inoperable anthracycline-resistant breast cancer. Int. J. Radiat. Oncol. Biol. Phys. 53, 1225–1233.

Insana, M.F., Hall, T.J., 1990. Parametric ultrasound imaging from backscatter coefficient measurements: image formation and interpretation. Ultrason. Imaging 12, 245–267.

Kaufmann, B.A., Lindner, J.R., 2007. Molecular imaging with targeted contrast ultrasound. Curr. Opin. Biotechnol. 18, 11–16.

Lee, J., Karshafian, R., Papanicolau, N., Giles, A., Kolios, Michael, C., Czarnota, Gregory, J., 2012. Quantitative ultrasound for the monitoring of novel microbubble and ultrasound radiosensitization. Ultrasound Med. Biol. 38, 1212–1221.

Lizzi, F.L., King, D.L., Rorke, M.C., Hui, J., Ostromogilsky, M., Yaremko, M.M., Feleppa, E.J., Wai, P., 1988. Comparison of theoretical scattering results and ultrasonic data from clinical liver examinations. Ultrasound Med. Biol. 14, 377–385.

Lizzi, Frederic, L., Astor, M., Liu, Tian, Deng, C., Coleman, D., Jackson, Silverman, R.H., 1997a. Ultrasonic spectrum analysis for tissue assays and therapy evaluation. Int. J. Imaging Syst. Technol. 8, 3–10.

Lizzi, Frederic, L., Feleppa, Ernest, J., Astor, M., Kalisz, A., 1997b. Statistics of ultrasonic spectral parameters for prostate and liver examinations. IEEE Trans. Ultrason. Ferroelectr. Freq. Control 44, 935–942.

Machado, J.C., Foster, F.S., 2001. Ultrasonic integrated backscatter coefficient profiling of human coronary arteries in vitro. IEEE Trans. Ultrason. Ferroelectr. Freq. Control 48, 17–27.

Madsen, E.L., Dong, F., Frank, G.R., Garra, B.S., Wear, K.A., Wilson, T., Zagzebski, J.A., Miller, H.L., Shung, K.K., Wang, S.H., Feleppa, E.J., Liu, T., O'Brien, W.D., Topp, K.A., Sanghvi, N.T., Zaitsev, A.V., Hall, T.J., Fowlkes, J.B., Kripfgans, O.D., Miller, J.G., 1999. Interlaboratory comparison of ultrasonic backscatter, attenuation, and speed measurements. J. Ultrasound Med. Off. J. Am. Inst. Ultrasound Med. 18, 615–631.

Oelze, M.L., O'Brien, William D., 2006. Application of three scattering models to characterization of solid tumors in mice. Ultrason. Imaging 28, 83–96.

Oelze, M.L., O'Brien, William, D., Blue, J.P., Zachary, J.F., 2004. Differentiation and characterization of rat mammary fibroadenomas and 4T1 mouse carcinomas using quantitative ultrasound imaging. IEEE Trans. Med. Imaging 23, 764–771.

Oelze, M.L., Zachary, J.F., 2006. Examination of cancer in mouse models using high-frequency quantitative ultrasound. Ultrasound Med. Biol. 32, 1639–1648.

Oelze, M.L., Zachary, J.F., O'Brien, William, D., 2002. Characterization of tissue microstructure using ultrasonic backscatter: theory and technique for optimization using a Gaussian form factor. J. Acoust. Soc. Am. 112, 1202–1211.

Partridge, S.C., Gibbs, J.E., Lu, Y., Esserman, L.J., Tripathy, D., Wolverton, D.S., Rugo, H.S., Hwang, E.S., Ewing, C.A., Hylton, N.M., 2005. MRI measurements of breast tumor volume predict response to neoadjuvant chemotherapy and recurrence-free survival. AJR Am. J. Roentgenol. 184, 1774–1781.

Sadeghi-Naini, A., Papanicolau, N., Falou, O., Tadayyon, H., Lee, J., Zubovits, J., Sadeghian, A., Karshafian, R., Al-Mahrouki, A., Giles, A., Kolios, Michael, C., Czarnota, , Gregory, J., 2013a. Low-frequency quantitative ultrasound imaging of cell death in vivo. Med. Phys. 40, 082901.

Sadeghi-Naini, A., Papanicolau, N., Falou, O., Zubovits, J., Dent, R., Verma, S., Trudeau, M.E., Boileau, J.F., Spayne, J., Iradji, S., Sofroni, E., Lee, J., Lemon-Wong, S., Yaffe, Martin, J., Kolios, Michael, C., Czarnota, Gregory, J., 2013b. Quantitative ultrasound evaluation of tumour cell death response in locally advanced breast cancer patients receiving chemotherapy. Clin. Cancer Res.

Schedin, P., O'Brien, J., Rudolph, M., Stein, T., Borges, V., 2007. Microenvironment of the involuting mammary gland mediates mammary cancer progression. J. Mammary Gland Biol. Neoplasia 12, 71–82.

Sethi, D., Garg, M., Khetarpal, S., Parshad, S., Sen, R., Sen, J., 2012. Histopathologic changes following neoadjuvant chemotherapy in various malignancies. Int. J. Appl. Basic Med. Res. 2, 111.

Smith, I.C., Heys, S.D., Hutcheon, A.W., Miller, I.D., Payne, S., Gilbert, F.J., Ah-See, A.K., Eremin, O., Walker, L.G., Sarkar, T.K., Eggleton, S.P., Ogston, K.N., 2002. Neoadjuvant chemotherapy in breast cancer: significantly enhanced response with docetaxel. J. Clin. Oncol. 20, 1456–1466.

Soliman, H., Gunasekara, A., Rycroft, M., Zubovits, J., Dent, R., Spayne, J., Yaffe, Martin, J., Czarnota, Gregory, J., 2010. Functional imaging using diffuse optical spectroscopy of neoadjuvant chemotherapy response in women with locally advanced breast cancer. Clin. Cancer Res. Off. J. Am. Assoc. Cancer Res. 16, 2605–2614.

Taggart, L.R., Baddour, R.E., Giles, A., Czarnota, Gregory, J., Kolios, Michael, C., 2007. Ultrasonic characterization of whole cells and isolated nuclei. Ultrasound Med. Biol. 33, 389–401.

Vlad, R.M., Alajez, N.M., Giles, A., Kolios, Michael, C., Czarnota, Gregory, J., 2008. Quantitative ultrasound characterization of cancer radiotherapy effects in vitro. Int. J. Radiat. Oncol. Biol. Phys. 72, 1236–1243.

Vlad, R.M., Brand, S., Giles, A., Kolios, Michael, C., Czarnota, Gregory, J., 2009. Quantitative ultrasound characterization of responses to radiotherapy in cancer mouse models. Clin. Cancer Res. 15, 2067–2075.

Yang, M., Krueger, T.M., Miller, James, G., Holland, M.R., 2007. Characterization of anisotropic myocardial backscatter using spectral slope, intercept and midband fit parameters. Ultrason. Imaging 29, 122–134.

Yao, L.X., Zagzebski, J.A., Madsen, E.L., 1990. Backscatter coefficient measurements using a reference phantom to extract depth-dependent instrumentation factors. Ultrason. Imaging 12, 58–70.